CrystEngComm

Accepted Manuscript

ROYAL SOCIETY OF CHEMISTRY

www.rsc.org/crystengcomm

Different interpenetrated coordination polymers based on flexible dicarboxylate ligands: topological diversity and magnetism

Jian-Qiang Liu[a*], Jian Wu[b*], Yao-Yu Wang[c], Jian-Tao Lin[a], Hiroshi Sakiyama[d]

Corresponding Authors: Dr. J. Q. Liu (Jianqiangliugdmc@126.com; Tel/Fax: 86-769-22896547)

Through tuning the nature of secondary ligands, ligand-to-metal molar ratio and metal ions, a family of entangled metal-organic frameworks have been prepared. This work evidently indicates that the effect of secondary ligands is critical in construction of these networks arrangement, which are also well regulated by the ligand-to-metal molar ratios and geometric preferences of metal centers. In addition, the stabilities of these compounds are discussed.

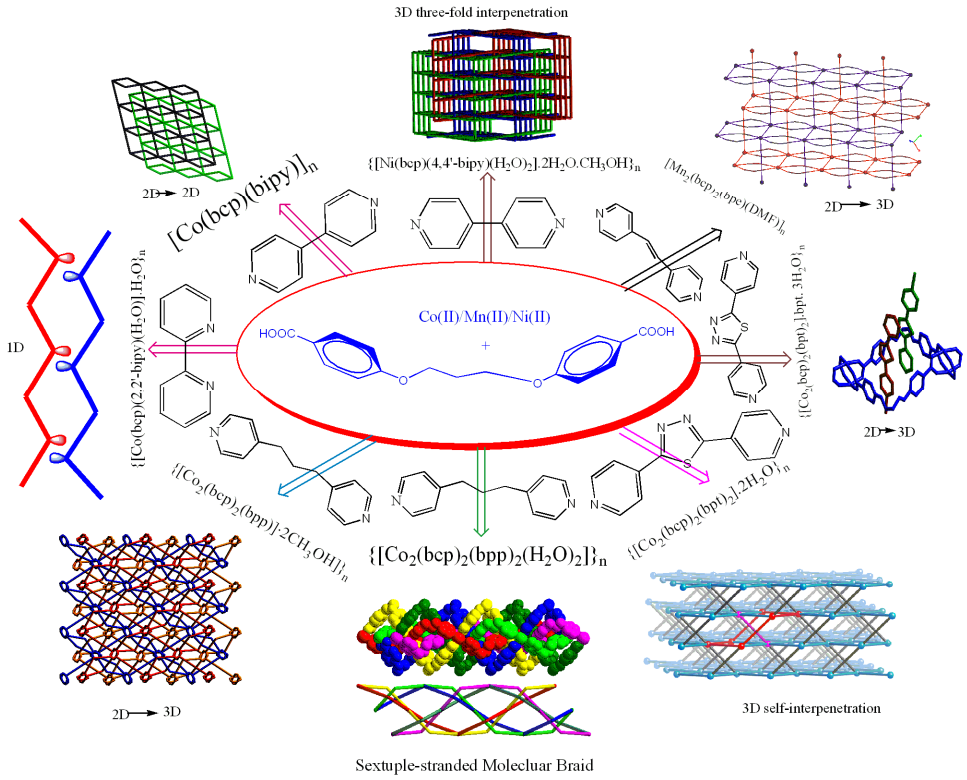

Different interpenetrated coordination polymers based on flexible dicarboxylate ligands: topological diversity and magnetism

Jian-Qiang Liu[a*], Jian Wu[b*], Yao-Yu Wang[c], Jian-Tao Lin[a], Hiroshi Sakiyama[d]

[a]Guangdong Medical College, School of Pharmacy, Dongguan, 523808, P. R. China; [b]Guangxi Key Laboratory of Chemistry and Engineering of Forest Products, Guangxi University for Nationalities, College of Chemistry and Ecological Engineering, Nanning, Guangxi 530006, China; [c]Key Laboratory of Synthetic and Natural Functional Molecule Chemistry of the Ministry of Education,Shaanxi Key Laboratory of Physico-Inorganic Chemistry, Northwest University, Xi'an 710069, PR China ;[d]Department of Material and Biological Chemistry, Faculty of Science, Yamagata University, Kojirakawa, Yamagata 990-8560, Japan

Corresponding Author: Dr. J. Q. Liu (Jianqiangliugdmc@126.com) and Dr. J. Wu (wujian2007gx@126.com)

Abstract

Through tuning the nature of secondary ligands, ligand-to-metal molar ratio and metal ions, three coordination polymers, namely $\{[Ni_2(bcp)_2(4,4'\text{-bipy})_2(H_2O)_4]\cdot 3.5H_2O\}_n$ (**1**), $\{[Co_2(bcp)_2(bpt)_2]\cdot 2.29H_2O\cdot bpt\}_n$ (**2**), $[Co_2(bcp)_2(bib)]_n$ (**3**) and $\{[Co(bcp)(2,2'\text{-bipy})(H_2O)]\cdot H_2O\}_n$ (**4**), have been synthesized and characterized. The structural feature of **1** shows 3D three-fold parallel interpenetrating framework with **$CdSO_4$** topology. In **2**, it exhibits a 2D→3D interpenetrating motif with pseudorotaxane. Compound **3** shows two identical 2D layers with $2^2.4^8.6^5$ topology that are interpenetrated in a parallel fashion, resulting in a twofold interpenetrating motif containing polyrotaxane and polycatenane character. However, a 1D zipper-like double-stranded chain is observed in polymer **4**. This work evidently indicates that the effect of secondary ligands and geometric preferences of metal centers are critical in construction of the resulting networks. In addition, the magnetic property was also discussed in compounds **2** and **3**.

Keywords: Carboxylate; Entangled structure; Magnetism

Introduction

The flourishing realm of crystal engineering has provided a sound junction between aesthetics of crystalline architectures and their potential functions. [1-5] Metal-organic frameworks with entangled motifs have attracted extreme concern for their intrinsic aesthetic appeal and properties. More specific types of entangled structures, such as polycatenation (*e.g.* Borromean), polythreading (*e.g.* polyrotaxane), and polyknotting (*e. g.* self-interpenetration), are of particular interest.[6] Many topologically interesting entangled structures have been discussed in comprehensive reviews.[1c,6a,6g,6h,6k] So at this point, much effort have mainly focused on the discovery of new entanglement patterns and understanding their formation mechanisms.[7-9]

Usually, entangled coordination polymers are formed by flexible and long organic ligands. For example, the V-shaped and flexible organic linkers (*e.g.* 4,4'-oxybis(benzoic acid)) take as a excellent building block and constructs different entangled motifs due to its flexuous geometry and various binding modes.[8] Thus, one effective way to modulate the type of entangled motif is to extend the flexibility and length of the ligand.[10] Recently, we have been interested in the syntheses and characterization of entangled MOFs containing the organic dicarboxylates of 4,4'-oxybis(benzoic acid) (H_2oba), 1,2-bis(4-carboxy-phenoxy)ethane(H_2bce) and 1,3-bis(4-carboxy-phenoxy)propane (H_2bcp).[10d,11] Among the three type of flexible dicarboxylate ligands, the segment of –O-X-O- chains are different with respect with the relative orientation of CH_2 groups. More interestingly, the employment of H_2bcp, Co(II) and bpp leads an unexceptional sextuple-stranded molecular braid.[10d] However, systematic investigation the coordination chemistry of H_2bcp has been rarely documented.[10d] On the other hand, the control of product architectures still remains a major challenge in this field, because the self-assembly process is frequently influenced by the type and spatial disposition of the ligand binding site, metal-to-ligand ratio, stereoelectronic preferences of the metal ion, and other factors.[12-14]

With this background in mind, we continued to our investigation and chose H_2bcp as a bridging ligand to react with the d-block metal ions in the presence of different

N-donor ligands. Three new coordination polymers, namely $\{[Ni_2(bcp)_2(4,4'\text{-bipy})_2(H_2O)_4]\cdot 3.5H_2O\}_n$ (**1**), $\{[Co_2(bcp)_2(bpt)_2]\cdot 2.29H_2O\cdot bpt]\}_n$ (**2**), $[Co_2(bcp)_2(bib)]_n$ (**3**) and $\{[Co(bcp)(2,2'\text{-bipy})(H_2O)]\cdot H_2O\}_n$ (**4**) (H_2bcp=1,3-bis(4-carboxy-phenoxy)propane, bpt=2,5-bis(4-pyridyl)-1,3,4-thiadiazole, 4, 4'-bipy =4,4'-bipyridine, bib=2,3-bis(4-pyridyl)butane and 2, 2'-bipy=2,2'-bipyridine), were designed and synthesized. Compound **1** exhibits 3D threefold **$CdSO_4$** topological net, polymer **2** has 2D polythreading architecture, Compound **3** shows two identical 2D layers with $2^2.4^8.6^5$ topology with polyrotaxane and polycatenane feature, and compound **4** shows a zipper-like double-stranded chain. The crystal structures and topological analyses of these compounds, along with a systematic investigation on the coordination modes of bcp ligand, metal ions and neutral ligand on the ultimate frameworks, will be represented and discussed in detail. Furthermore, the magnetic property was also discussed in compounds **2** and **3**.

Experimental

Materials and Method

All reagents were purchased from commercial sources and used as received. IR spectra were recorded with a Perkin–Elmer Spectrum One spectrometer in the region 4000–400cm^{-1} using KBr pellets. TGA were carried out with a Metter–Toledo TA 50 in dry dinitrogen (60mL.min^{-1}) at a heating rate of 5°C min^{-1}. X-ray powder diffraction (XRPD) data were recorded on a Rigaku RU200 diffractometer at 60KV, 300mA for *Cu* K_α radiation (λ = 1.5406 Å), with a scan speed of 2 °C/min and a step size of 0.02° in 2θ. Magnetic susceptibility data of powdered samples restrained in parafilm were measured on Oxford Maglab 2000 magnetic measurement system in the temperature range 300–1.8 K and at field of 1KOe.

X-ray Crystallography: Single crystal X-ray diffraction analyses of the four compounds were carried out on a *Bruker SMART APEX II CCD* diffractometer equipped with a graphite monochromated Mo$K\alpha$ radiation (λ = 0.71073 Å) by using ϕ/ω scan technique at room temperature. The intensities were corrected for Lorentz and polarization effects as well as for empirical absorption based on multi-scan techniques; all structures were solved by direct methods and refined by full-matrix

least-squares fitting on F^2 by SHELX-97.[15] Absorption corrections were applied by using multi-scan program SADABS.[16] Non-hydrogen atoms were refined anisotropically. It was assigned to some non-hydrogen atoms an isotropic temperature factor of 1.3 times the isotropic temperature factor of the atom to which they were attached. The hydrogen atoms of organic ligands were placed in calculated positions and refined using a riding on attached atoms with isotropic thermal parameters 1.2 times those of their carrier atoms. The water hydrogen atoms were located from difference maps and refined with isotropic thermal parameters 1.5 times those of their carrier atoms. The hydrogen atoms of lattice water molecules in compound **1**and **2** were not located using the different Fourier method. The entire disordered water molecule O3W, O4W, O5W, O6W, and O7W have the occupancies of 0.25 in compound **1**. The disordered water molecule O13 has the occupancy of 0.77 and 0.23, and O14 has the occupancy of 0.52 and 0.48 in compound **2**, respectively. The disordered water molecule O2W has the occupancy of 0.50 and 0.50 in compound **4**. The available crystals of the compound **2** diffracted very weakly, especially at higher diffraction angles. This is most likely related to the disorder in the solvent molecule. Namely, the crystal quality and data in **2** was not good enough so a sufficient fraction of the unique data is above the 2 sigma level. The crystal quality was not good. After several attempt of data collection, the reported one is found to be the best one. Thus, more restraints were applied during refinement of the structures including distance restraints and thermal restraints which have been used in some unreasonable atoms in order to permit acceptable refinement of these parameters in compounds. Table 1 shows crystallographic data of **1**–**4**. Selected bond distances and bond angles, parameters are listed in Table 2. Selected bond distances and angles of hydrogen bonds are given in Table S1. **CCDC**: 913913-913915 for **1,2,4**, and 971937 for **3**.

Synthesis of these complexes

$\{[Ni_2(bcp)_2(4,4'\text{-bipy})_2(H_2O)_4]\cdot 3.5H_2O\}_n$ (**1**)

A mixture of $NiSO_4\cdot 7H_2O$ (0.026g, 0.1mmol), H_2bcp (0.032g, 0.1mmol), 4,4'-bipy (0.012g, 0.1mmol), CH_3OH (2mL) and deionised water (10mL) was stirred for 30min in air. The pH of the resulting solution was adjusted to 7 using dilute NaOH (0.1mol/L)

and kept at 150 ℃ for 72h at oven, and then cooled down to 25 ℃. The resulting crystals formed were filtered off, washed with water and dried in air. $C_{54}H_{59}N_4Ni_2O_{19.5}$ (1193.48). Calcd: C, 54.34; H, 4.98; N, 4.69. Found C, 54.01; H, 4.77; N, 4.50. **IR** (KBr, cm^{-1})**:** 3389(s), 2982(m), 2768(w), 2035(w), 1599(m), 1408(vs), 1266(m), 1138(w), 1011(m), 988(w), 866(w), 759(m), 658(s).

$\{[Co_2(bcp)_2(bpt)_2]\cdot 2.29H_2O\cdot bpt\}_n$ (**2**)

The synthesis procedure of **2** is similar to that for **1**, except that bipy and $NiSO_4\cdot 7H_2O$ were replaced by bpt (0.1mmol) and $CoSO_4\cdot 7H_2O$ (0.1mmol), respectively. $C_{70}H_{56.58}Co_2N_{12}O_{14.29}S_3$(1508.55) Calcd: C, 55.73; H, 3.78; N, 11.14. Found C, 55.26; H, 4.12; N, 11.22. **IR** (KBr, cm^{-1})**:** 3320(s), 2997(m), 2332(w), 1988(w), 1612(vs), 1452(vs), 1208(m), 997(w), 822(s), 721(m), 659(w), 577(w).

$[Co_2(bcp)_2(bib)]_n$ (**3**)

The synthesis procedure of **3** is similar to that for **2**, except that bipy was replaced by bib (0.11mmol). $C_{48}H_{44}Co_2N_2O_{12}$ (958.71). Calcd: C: 60.13; N: 2.92; H: 4.63. Found: C: 55.81; N: 2.69; H: 5.01. **IR** (KBr, cm^{-1}): 3072(m); 1605(vs); 1542(vs); 1419(vs); 1248(vs); 1162(s); 1046(m); 789(vs); 650(m).

$\{[Co(bcp)(2,2'\text{-bipy})(H_2O)]\cdot H_2O\}_n$ (**4**)

The synthesis procedure of **4** is similar to that for **2** except that bpt is replaced by 2,2'-bipy (0.1mmol). $C_{27}H_{26}CoN2O_8$(565.43). Calcd: C, 57.35; H, 4.63; N, 4.95. Found C, 57.33; H, 4.68; N, 5.01. **IR** (KBr, cm^{-1})**:** 3350(m), 2998(w), 2128(w), 1899(w), 1672(vs), 1432(vs), 1245(m), 898(w),778(m), 648(w), 558(w).

Results and Discussion

$\{[Ni_2(bcp)_2(4,4'\text{-bipy})_2(H_2O)_4]\cdot 3.5H_2O\}_n$ (**1**)

The asymmetric unit of **1** contains two independent Ni atoms (in special position), one bcp ligand (in general position), two 4,4'-bipy ligands and two independent coordinative water molecules (in general position), and some lattice water molecules. The bcp adopts bis(monodentate)[(k^1)-(k^1)-μ_2] mode (Schem.1c). Each Ni(II) is coordinated by two *trans* 4,4'-bipy ligands, two *trans* bcp ligands, and two *trans* water molecules, to give an octahedral geometry (Fig.1a). Furthermore, the water molecules bond to the uncoordinated oxygen atoms of the carboxylate ligands. The Ni-O/N bond

lengths are within the normal range. Both the 4,4'-bipy and bcp ligands simultaneously bridge adjacent two metal ions in two direction, thus, a 3D coordination polymer is produced (Fig. 2a). The metal atoms essentially act as 4-connecting nodes, and the network has **$CdSO_4$** $\{(6^5.8)$ *vs* $[6.6.6.6.6(2).*]\}^1$ topology (Fig. 2b).[17-20] The spaciousness of the net leads to the interpenetration of three identical nets (Fig. 2c). The nets are crosslinked by extensive hydrogen bonding between water molecules and the uncoordinated carboxylate oxygen atoms.

/Insert Fig. 1 and Fig. 2/

$\{[Co_2(bcp)_2(bpt)_2]\cdot 2.29H_2O\cdot bpt\}_n$ (**2**)

The structural unit contains two unique Co(II) atoms, two bcp ligands, two coordinative bpt ligands, one free bpt ligand and 2.29 lattice water molecules (Fig. 1b). The bcp adopts a $(k^1\text{-}k^1)\text{-}(k^1\text{-}k^1)\text{-}\mu_4$ fashion and connects neighboring Co(II) ions(Scheme. 1b), forming a $Co_2(RCO_2)_4$ paddle-wheel units. However, the Co atoms don't lie opposite each other across the dimer, as they would in *e.g.* a $Cu_2(RCO_2)_4$ dimer, but rather are offset, with weaker interactions to oxygen atoms on the opposite side of the dimer. The cobalt atoms are bridged into dimers by the carboxylate groups of four different bcp ligands; these ligands adopt a V-shaped conformation and thus the dimers are bridged into 1D chains containing large 'loops' between the dimers (Fig. 2b). The square pyramidal geometries of the metal atoms are completed by monodentate bpt ligands which lie in the axial site and project above and below the chains; the different sides of the chains contain crystallographically different bpt ligands .

The chains are arranged in sheets (Fig. 3a), and these sheets are arranged such that the monodentate bpt ligands project into the loops of chains in the adjacent sheets on either side of it. Each sheet has one close neighbor through which its bpt ligands project such that the coordinated pyridyl groups are roughly level with the loops in the adjoining sheet (Fig. 3b). The sheet on the other side is further away, and here the interdigitation occurs such that the uncoordinated pyridyl sets are level with the adjoining sheet loops. This larger separation creates square channels in which lie the uncoordinated water molecules and intercalated bpt molecules (Fig. 3b). Each loop of

each chain is thus penetrated by two bpt ligands from adjoining chains, in which results in new twofold 2D→3D polythreaded architecture (Fig. 3c). Recently, we have reported a new compound of $\{[Cu_4(oba)_4(bpt)_2(H_2O)_3]\cdot 6H_2O\}_n$.[10h] The structure of the Cu(II) compound exhibits a fascinating 2D→3D polythreaded architecture, which contains a side arm of bpt in one layer involving nine polymeric units at a time. Interestingly, if hydrogen bonds are taken into account, the resulting structure displays a 5-fold interpenetrated 3D **mot** topological framework. The difference between the **2** and $\{[Cu_4(oba)_4(bpt)_2(H_2O)_3]\cdot 6H_2O\}_n$ suggests that the coordinative mode of bpt may play an important role in modulating the interpenetrated character.

$[Co_2(bcp)_2(bib)]_n$ (**3**)

The structure of **3** contains one unique Co atom, half unique bib and one unique bcp ligand. The Co(II) atom is coordinated by four oxygen atoms from two adjacent bcp ligands and one nitrogen atom to provide the square-pyramidal geometry. However, Co1 could be considered to have octahedral coordination if the second Co1-O6 bond of 2.293 Å was taken into account (Fig. 1c). The Co-O/N bond lengths are within the normal range. The bcp adopts a $(k^1\text{-}k^1)\text{-}(k^1\text{-}k^1)\text{-}\mu_4$ fashion. Two crystallographycially equivalent Co(II) atoms are linked by four carboxylate groups of bcp using bis(bidentate) mode to give a paddle-wheel unit of $[Co_2(CO_2)_4]$ fragment in which the Co···Co distance is 2.878(4) Å. These dimers are connected *via* the backbones of the bcp ligands such that each pair of adjoining dimers is connected by two bcp ligands, in which result in the 'loops' motif. These chains are then crosslinked by 4,4'-bipy ligands, which bond to the axial positions of the dimers and create the (4,4) sheet (Fig.4a).

Pairs of sheets interpenetrate in a 2D→2D parallel fashion, as shown in Fig. 4b. The interpenetration is such that each metal-bcp loop has a flexible bib ligand from the other net passing through it. The sheets individually can be described as having (4,4) topology, however, this description simplifies the loops into a single linkage and thus becomes inadequate for describing the interpenetration (Fig. 4c). Thus, the net could be better described as 6-connected $2^2.4^8.6^5$ topology containing polyrotaxane and polycatenane feature (Fig.4d -4e).[11e]

{[Co(bcp)(2,2'-bipy)(H_2O)]·H_2O}$_n$ (**4**)

It has been noted that aromatic chelating ligands (such as 2,2'-bipy and 1,10-phen) often lead to low dimensional polymers and may provide potential supramolecular recognition sites for π–π aromatic stacking interactions to form multi-stranded helices.[22] In the structure of **4**, there is one Co^{II} atom, one bcp ligand, and one 2,2'-bipy ligand, one coordinated water molecule and one lattice water molecule in each unit (Fig. 1d). Each Co^{II} atom in **4** is primarily coordinated by three oxygen atoms from two carboxylate groups of adjacent bcp ligands and one coordinated water molecule, and two nitrogen atoms from a chelating 2,2'-bipy to furnish a distorted octahedral geometry. Each pair of adjacent Co^{II} atoms is bridged by bcp ligands to form a chain running along the *b*-direction with a long pitch of 16.3 Å (Fig. 5a). These chains are further extended into two-dimensional (2D) networks through interdigitation of the lateral 2,2'-bipy ligands from adjacent chains (Fig. 5b). The offset fashion with a face-to-face distance is 3.76(8) Å, indicating aromatic π–π stacking interactions (Fig. 5c).[22] To the best of our knowledge, such zipper-like double-stranded helical chains have been documented in some examples.[23] The double-stranded helical chain is stabilized by hydrogen bond interactions between the uncoordinated oxygen atoms of carboxylate groups and the water molecules.

/Fig. 3, Fig. 4 and Fig. 5/

Comparison of the structures of coordination polymers

The simultaneous use of the N-donors and aromatic V-shaped dicarboxylate ligands affords diverse entangled networks. Herein, we systematic explored the coordination chemistry of bcp ligand, and constructed some new entangled motifs in our group, as concluded in Scheme. 2. Although we are unable to propose definitive reasons as to why the compounds exhibit different topologies with our present state of knowledge, some of the general trends observed are discussed below.

Effect of secondary ligand:

The polymers are strongly related to the secondary ligand. The following discussion provides a qualitative explanation for this conclusion. Although the 4,4'-bipy, 2,2'-bipy, bpt and bib ligands are all neutral N-containing linkages, they are quite

different. For example, the bpt has an angular disposition of its terminal pyridyl spacers due to its central thiadiazole ring and two more potential N-donor atoms, which may favor to construct the unexpected and unpredictable motifs.[13,24] Recently, we have reported one new entangled compound of $\{[Co_2(bcp)_2(bpt)_2 \cdot 2H_2O]\}_n$, which shows 3D 6-connected net with $2^2.4^8.6^5$ topology containing polyrotaxane character and unusual self-penetrating topology.[10h] For instance, the bpt taking a monodentate mode binds to metal center in **2**, whereas for **1**, the 4,4'-bipy adopts bridging mode to extend the full network. The free bpt ligand in compound **2** may be one of the important factors for the construction of the structure as it might function as templates and occupy the pores, thus preventing higher dimensional network. Furthermore, the existence of coordinated water molecules in complex **1** is also one important factor in inducing the coordinative mode of bcp. The different feature of neutral ligand in **1** and **2** may explain the different coordination of bcp ligand. These feature leads to the formation of completely different coordination architectures in **1** and **2**. While in **2** and **3**, although bcp and metal center have the similar coordinative modes, the resulting network are different. The difference may be caused by the different intrinsic skeletons between bpt and bib. In compounds **1** and **3**, the N-donor ligands of 4,4'-bipy and bib shows bis(monodentate) fashion, the sizes of backbones are different. Thus, only a molecular ring of $[Co(bcp)]_n$ is observed in **3**. To further examine the influence of the secondary ligand on the self-assembly entities, a aromatic chelating ligand 2,2'-bipy was introduced into Co-bcp system. Consequently, compound **4**, featuring zipper-like chain structure, was obtained. The neighboring chains make double-stranded chains through supramolecular recognition. This could be related to the fact that chelating ligands such as 2,2'-bipy serve as a "passive" role in occupying coordinative sites on metal centers and produce steric constrains.[8a] Comparing the neutral ligands in **1** and **3**, the difference is the position of the pyridyl ring. The 2,2'-bipy ligand has a comparatively large steric hindrance, which may decrease the ability of coordination to metal ion and result in the low dimensional network. The V-shaped and flexible carboxylate ligand bcp is also fundamental for the construction of chains in the presence of terminal ligands such as phen and

2,2'-bpy, while the linear ligands bpt and 4,4'-bipy contribute to higher dimensionalities in complexes **1** and **2**, thus showing that the shape of the ligands plays an important role in the architecture of complexes. Thus, the ancillary ligand has a significant effect on the formation and structure of the coordination polymers. In order to construct peculiar topological polymers, an effective method can be to introduce different ancillary ligands.

Effect of metal nature:

It is interesting that, although **1** and $\{[Co(bcp)(4,4'\text{-}bipy)_{0.5}]_n$ bind to the same organic ligands, the Co^{II} and Ni^{II} complexes give completely different products.[11e] From the above description, the compound dimeric Co(II) unit exhibits 6-connected nets with $2^2.4^8.6^5$ topology containing polyrotaxane character, while the compound **1** only has one metallic unit and shows three-fold interpenetrating **$CdSO_4$** topological motif. Furthermore, the Co(II) and Ni(II) ions have the similar distorted octahedral geometries, but their coordination environments are different. In compound of $\{[Co(bcp)(4,4'\text{-}bipy)_{0.5}]_n$, there are two bis(bidentate) bcp and two 4,4'-bipy ligands around the metal ions, whereas in complex **1**, which contains two bis(monodentate) bcp ligands, two 4,4'-bipy ligands and two terminal water molecules around the metal ions. More ligands surround each Co(II) ion than that of the Ni(II) ion. We also reported a polymer of $\{[Mn_2(bcp)_2(bpe)(DMF)]\}_n$, which contains tetranuclear subunit and shows 2D→3D inclined interpenetration motif with polyrotaxane character.[25] The results indicate that the metal radius may promote interpenetration and higher dimensionality. Similar results are found for the other complexes with related dicarboxylate ligands.[26] A rational assembly of metal ions is critical for the formation of novel and higher dimensional networks.

Ligand-to-metal molar ratio:

Two distinct structures of two compounds $\{[Co_2(bcp)_2(bpp)_2(H_2O)_2]\}_n$ and $\{[Co_2(bcp)_2(bpp)]\cdot 2CH_3OH]\}_n$ were reported in our recent communication.[13] The former compound shows an unique interlaced sextuple-stranded molecular braid, which is interwoven by three double-stranded *meso*-helices. When the ligand: metal molar ratio is 2:1, the structure of the latter set undergoes a 2D sheet, which reveals a

three-fold 2D→3D parallel interpenetrating motif. A compound of $\{[Co_2(bcp)_2(bpt)_2\cdot 2H_2O]\}_n$, with metal-ligand stoichiometry of 1:1, exhibits **Pcu** motif containing unusual self-penetrating topology,[19d] whereas polymer **2**, with a Co(II): bpt stoichiometry of 1:0.5, adopts 2D→3D polythreaded architecture. Not surprisingly, the multimodal ligand, with an enhance number of donor atoms, was particularly sensitive to the metal-to-ligand ratio.[11a]

Condition of the syntheses

The pH values of the reaction solutions play a role key in determining the final products. The pH values of the reaction solutions will be signification decreased after crystallization of complexes **1-4**, whereas for $\{[Co_2(bcp)_2(bpp)_2(H_2O)_2]\}_n$, it is slightly higher pH value (ca. 7.5).[13] A possible explanation for this observation is that the isolation of complexes **1-3** incorporation of rigid N- donor component will affect relevant the solution concentration of basicity. Moreover, with regard to other metal ions (Co(II) and Mn(II)), such a pH effect on the assembly is not valid, indicating its specific selectivity to Ni(II).[11, 13, 25,19d]

As discussed above, a variety of framework structures can be achieved on the basis of the choice of secondary ligands, ligand-to-metal molar ratio and metal ions. However, all the variable factors cannot be accurately forecasted at this stage.

/Scheme 1 and Scheme 2/

Thermogravimetric Analyses and XRPD

To study the stabilities of the polymers, thermogravimetric analyses (TGA) of complexes **1-4** were performed (Fig. S1). The compound **1** shows two of weight loss steps. The first weight loss began at 20°C and completed at 208°C. The observed weight loss of 8.8% is corresponding to the loss of the water molecules (calcd 7.37%). The second weight loss occurs in the range 230−539°C, which can be attributed to the elimination of bipy and bcp ligands. The compound **2** also has two observed weight loss, first weight loss of 19.2% is corresponding to the loss of the crystallization water and free bpt (calcd 18.6%). A gradual weight loss from 251 °C dictates that the complex was decomposing continuously when the temperature was rising up. The 20.4% mass remnant at 336 °C is consistent with CoO (22.1 % predicted). The

compound **3** shows one of weight loss step. The mass of **3** remains largely unchanged until the decomposition onset temperature of ca. 360 °C. All removal of organics was completely by 770 °C, indicated by a further weight loss, roughly consistent with expulsion of the bcp and bib ligands. The compound **4** also has two observed weight loss, first weight loss of 6.4% is corresponding to the loss of the crystallization water and coordinated water molecule (calcd 7.1 %). A precipitous weight loss of 79.5 % was completed by 805 °C, corresponding to fracture of the net with the expulsion of all organic ligands.

Additionally, to confirm the phase purity of compounds, the original samples were characterized by X-ray powder diffraction (XRPD) at room temperature. The patterns that were simulated from the single-crystal X-ray data of compounds were in agreement with those that were observed (Fig. S2).

Magnetism

The $\chi_A T$ value for **2** was 3.31 cm^3 K mol^{-1} at 300 K, and this is much larger than the spin only value (1.88 cm^3 K mol^{-1}) for the S = 3/2 state, but close to the value (3.38 cm^3 K mol^{-1}) when the spin and orbital moment exist independently. When decreasing the temperature, the $\chi_M T$ decreases gradually and reaches a local minimum (0.24 cm^3 K mol^{-1}) at ~20 K. In the χ_M *versus* T plot, the local maximum was observed at ~210-220 K, and this indicates the antiferromagnetic interaction between Co ions in the paddle-wheel dimer (Fig. 6a). When the data above 150 K were analyzed using a dimer model,[28] the J value was estimated as ~−76 cm^{-1}. However, the behavior below 50 K cannot be explained by the dimer model. In the χ_M versus T plot, the local minimum was observed at ~50 K, and χ_M increased significantly below ~20 K; in the $\chi_M T$ versus T plot, a local maximum (0.46 cm^3 K mol^{-1}) is observed at ~10 K. If the 1-dimensional alternating chain model is used, the parameters were obtained as follows; J = −77.5 cm^{-1}, λ = −173 cm^{-1}, κ = 0.90, v = −0.13 cm^{-1}, TIP = 0.0018 cm^3 mol^{-1}, angle = 24°, J' = −2.0 cm^{-1}, α = 0.80 and the agreement factor $R = 8.6\times10^{-4}$. That means that it is an alternating chain with J_1 = −140 cm^{-1} and J_2 = −16 cm^{-1}, and the increase in χ_M below 50 K may be due to the dimensionality (Fig. 6a). In this simulation, antiferromagnetic interaction between

chains were considered, and the interaction per one Co was estimated as $J' = -2.0$ cm^{-1}; although the fitting quality below 20 K was not satisfactory, the decrease in $\chi_A T$ below 10 K may be due to the antiferromagnetic interaction between the chains. The angle (24°) corresponds to the crystal structure (22.1°) well. The obtained TIP value seems to be large, but this may be due to the higher states with orbital angular momentum. The -2J value of **2** is in the normal range for the dinuclear cobalt-carboxylate complexes.[28]

The $\chi_M T$ value per dinuclear cobatt(II) unit in **3** was 6.24 cm^3 K mol^{-1} at 300 K, and this is much larger than the spin only value (3.75 cm^3 K mol^{-1}) for the $S = 3/2$ state, but close to the value (6.75 cm^3 K mol^{-1}) when the spin and orbital momenta exist independently. When decreasing the temperature, the $\chi_A T$ decreases gradually and reaches a minimum (0.22 cm^3 K mol^{-1}) at 2.0 K. In the χ_M versus T plot, the local maximum was observed at ~10 K, and this indicates the antiferromagnetic interaction between Co ions in the dinuclear unit. When the data was analyzed using a dimer model [28], the parameters were obtained as follows: $J = -5.9$ cm^{-1}, $\lambda = -107$ cm^{-1}, $\kappa = 0.66$, $v = 4.29$ cm^{-1}, $\theta = -0.66$ K, TIP = 0.0018 cm^3 mol^{-1} and the agreement factor $R = 6.1\times10^{-4}$. As shown in Fig. 6b.

It is well-know that for exchange interaction in these molecules, a superexchange mechanism governs a main metal-metal interaction, in which the electronic structure of the bridging of the O-C-O moiety determines the magnitude of the antiferromagnetic interaction. The parameter Φ_{bend} of the Co-O-C-O-Co is very important. It is well-know that the larger Φ_{bend} could generate a larger decrease in -2J because of reduced overlap of the Co d_{x2-y2} orbital with the 2px carboxylate oxygen orbital in the symmetric HOMO.[29] In the case of **2**, the Φ_{bend} is 11.5(3)°, which is slightly smaller than that of $[Co_2(oba)_2(bib)\cdot H_2O]$. and larger than that observed for $[Co_3(oba)_3(bpmp)_2]$.[29c] According to the structure of compound **2**, it could be presumed that the main magnetic interactions between the paddle-wheel unit metal centers, while the superexchange interactions between Co ions through the bcp bridge can be ignored due to the length of the bcp ligands.

/Insert Fig. 6 /

Conclusion

In conclusion, we have presented a rational synthetic strategy that successfully achieved a family of interesting polymeric entangled compounds by a combination of flexible dicarboxylate ligand and different N-donor ligands. Although the resulting structural motifs are impossible to predict with our present state of knowledge, the strategy reveals a potential approach for rational design of entangled systems with long flexible ligands. Accordingly, this present findings herein will further enrich the crystal engineering strategy and offer the possibility of modulating the formation of desired solid-state materials.

Acknowledgments

This work was partially supported by the grants from the National Natural Science Foundation of China (21201044), Natural Science Foundation of Guangdong Province(S2012040007835), Training plan of Guangdong Province outstanding young teachers in Higher Education Institutions, Foundation for Distinguished Young Talents in Higher Education of Guangdong Province (LYM11069),Guangxi University for Nationalities (2011DQ022), Technologies R & D program of Zhanjiang (2011C3108013 and 2012C3106016), Science & Technology Innovation Fund of Guangdong Medical College (STIF201112) and greater contribution from Prof. S. R. Batten and Zeller. Matt.

References:

(1) (a) B.Moulton and M. J. Zaworotko, *Chem. Rev*., 2001, **101**, 1629; (b) H.X. Deng, C. J.Doonan, H. Furukawa, R. B. Ferreira, J.Towne, C. B. Knobler, B. Wang and O. M. Yaghi, *Science*, 2010, **327**, 846; (c) X. M.Zhang, Z. M.Hao, W. X. Zhang and X. M. Chen, *Angew. Chem., Int. Ed*., 2007, **46**, 3456.

(2) (a) S. Horika, S. Shimomura and S. Kitagawa, *Nature. Chem*., 2009, **1**, 695; (b) C. J. Doonan, D. J. Tranchemontagne, T. G. Glover, J. R. Hunt and O. M. Yaghi, *Nature. Chem*., 2010, **2**, 235; (c) Y. Qi, F.Luo,Y.X. Che and J. M. Zheng, *Cryst. Growth Des*., 2008, **8**, 606; (d) S. Q. Ma, J. Eckert, P. M. Forster, J.Yoon, Y. K.Hwang, J. S. Chang, C. D. Collier, J. B. Parise and H. C. Zhou, *J. Am. Chem. Soc*., 2008, **130**, 15896. (e) L. F. Ma, L. Y. Wang, M.Du and S. R. Batten, *Inorg. Chem*., 2010, **49**, 365. (f) L. F. Ma, B. Liu, L. Y. Wang, C. P. Li and M. Du, *Dalton Trans*., 2010, **39**, 2301. (g) L. F.Ma, Q. J. Meng, C. P.Li, B.Liu, L. Y. Wang, M. Du and F. P. Liang, *Cryst. Growth Des*., 2010, **10**, 3036.

(3) (a) M. Dinca, A. F. Yu and J. R. Long, *J. Am. Chem. Soc*., 2006, **128**, 8904; (b) C. D. Wu, A.Hu, L. Zhang and W. B. Lin, *J. Am. Chem. Soc*., 2005, **127**, 8940; (c) A. C. McKinlay, R. E. Morris, P. Horcajada, G. Férey, R. Gref, P. Couvreur and C. Serre, *Angew. Chem., Int. Ed*., 2010, **49**, 6260.

(4) (a) C. S. Liu, X. S. Shi, J. R. Li, J. J. Wang and X. H. Bu, *Cryst. Growth Des*., 2006, **6**, 656; (b) R. Q. Zou, H. Sakurai and Q. Xu, *Angew. Chem., Int. Ed*., 2006, **45**, 2542.
(5) (a) B. F. Abrahams, S. R. Batten, H. Hamit, B. F. Hoskins and R. Robson, *Angew. Chem., Int. Ed*., Engl. 1996, **35**, 1690; (b) S. R. Batten and K. S. Murray, *Coord. Chem. Rev*., 2003, **246**, 103; (c) H. Y. An, E. B. Wang, D. R. Xiao, Y. G. Li, Z. M. Su and L. Xu, *Angew. Chem., Int. Ed. Engl*., 2006, **45**, 904; (d) D. L.Long, R. J. Hill, A. J. Blake, N. R. Champness, P. Hubberstey, C. Wilson and M. Schröder, *Chem. Eur. J.,* 2005,**11**, 1384; (e) X. N. Cheng, W. X. Zhang and X. M. Chen, *CrystEngComm,* 2011, **13**, 6613.
(6) (a) L. Carlucci, G. Ciani and D. M. Proserpio, *Coord. Chem. Rev*., 2003, **246**, 247; (b) S. R. Batten, *CrystEngComm*, 2001, **3**, 67; (c) S. R. Batten and R. Robson, *Angew. Chem. Int. Ed*., 1998, **37**, 1460 (d) V. A. Blatov, L. Carlucci, G. Ciani and D. M. Proserpio, *CrystEngComm*, 2004, **6**, 378; (e) L. Carlucci, G. Ciani, M. Moret, D. M. Proserpio and S. Rizzato, *Angew. Chem. Int. Ed*., 2000, **112**, 1566.
(7) (a) X. L.Wang, C.Qin, E. B. Wang, L. Xu, Z. M. Su and C. W. Hu, *Angew. Chem., Int. Ed. Engl*. 2004, **46**, 5146; (b) D. R. Xiao, E. B. Wang, H. Y. An, Y. G. Li, Z. M. Su and C. Y. Sun, *Chem. -Eur. J*., 2006, **12**, 6528; (c) X. L. Wang, C. Qin, E. B.Wang and Z. M. Su, *Chem. -Eur. J*., 2006, **12**, 2680.
(8) (a) F. Y. Lian, F. L. Jiang, D. Q. Yuan, J. T. Chen, M. Y. Wu and M. C. Hong, *CrystEngComm*, 2008, **10**, 905 ; (b) Y. L.Wei, H. W. Hou, L. K. Li, Y. T. Fan and Y. Zhu, *Cryst. Growth Des*., 2005, **5**, 1405.
(9) (a) J. Z. Hou, M. Li, Z. Li, S. Z. Zhan, X. C. Huang and D. Li, *Angew. Chem., Int. Ed*., 2008, **47**, 1711; (b) A. L. Cheng, N. Liu, Y. F. Yue, Y. W. Jiang, E. Q. Gao, C. H. Yan and M. H. He, *Chem. Commun*., 2007 407; (c) K. L. Mulfort, O. K. Farha, C. D. Malliakas, M. G. Kanatzidis and J. T. Hupp, *Chem. Eur. J*., 2010, 16, 276; (d) T. H. Noh, Y. J. Choi, Y. K. Ryu, Y. A.Lee and O. S. Jung, *CrystEngComm*, 2009, **11**, 2371; (e) J. Xu, Z. S. Bai, M. S. Chen, Z. Su, S. S. Chen and W.Y. Sun, *CrystEngComm*, 2009, **11**, 2728; (f) D. B. Amabilino and L. Pérez-García, *Chem. Soc. Rev*., 2009, **28**, 1562; (g) S. N.Wang, J. F. Bai, Y. Z. Li, M. Scheer and X. Z.You, *CrystEngComm*, 2007, **9**, 228.
(10) (a) B. L. Chen, S. C. Xiang and G. D. Qian, *Acc. Chem. Res*. 2010, **43**, 111; (b) P. Mahata, A. Sundaresan and S. Natarajan, *Chem. Commun*, 2007, 4471; (c) X. M. Chen and G. F. Liu, *Chem.–Eur. J*., 2002, **8**, 4811; (d) J. Q. Liu, Y. Y.Wang, L. F. Ma, G. L. Wen, Q. Z. Shi, S. R. Batten and D. M. Proserpio, *CrystEngComm*, 2008, **10**, 1123; (e) C. Y. Sun, S. Gao and L. P. Jin, *Eur. J. Inorg. Chem*., 2006, 2411; (f) S. Pramanik, C. Zheng, X. Zhang, T. J. Emge and J. Li, *J. Am. Chem. Soc*., 2011, **133**, 4153; (g) X. L. Wang, C. Qin, E. B. Wang, Y. G. Li, Z. M. Su, L. Xu and L. Carlucci, *Angew. Chem., Int. Ed*. 2005, **44**, 5824; (h) L. G. Wen, Y. Y. Wang, Y. N. Zhang, G. P. Yang, A. Y. Fu and Q. Z. Shi, *CrystEngComm*, 2009, **11**, 1519.
(11) (a) J. Q. Liu, Y. Y. Wang, P. Liu, Z. Dong, Q. Z. Shi and S. R. Batten, *CrystEngComm*, 2009, 11, 207; (b) J. Q. Liu, Y. Y. Wang, Y.N. Zhang, P.Liu, Q. Z. Shi and S. R. Batten, *Eur. J. Inorg. Chem*., 2009, 147; (c) J. Q. Liu, Y. Y. Wang and Z. B.Jia *Inorg. Chem. Commun*., 2011, **14**, 519; (d) J. Q. Liu, Y. Y. Wang and Y. S. Huang, *CrystEngComm*, 2011, **13**, 3733; (e) J. Wu, J. Q. Liu, G. Z. Ping, D. H. Xu and S. Hiroshi, *Inorg. Chem. Commun*., 2012, **25**, 10.
(12) B. Lippert and P. J. Miguel, *Chem. Soc. Rev*., 2011, **40**, 4475.
(13) (a) J. J. M. Amoore, C. A. Black, L. R. Hanton and M. D. Spicer, *Cryst. Growth Des*., 2005, **5**, 1255; (b) F. Y. Cui, K. L. Huang, Y. Q. Xu, Z. G. Han, X. Liu, Y. N. Chi and C. W. Hu,

CrystEngComm, 2009,**11**, 2757.
(14) (a) B. C. Tzeng, T. H. Chiu, B. S. Chen and G. H. Lee, *Chem. –Eur. J*. 2008, **14**, 5237; (b) R. Banerjee, A. Phan, B.Wang, C. Knobler, H.Furukawa, M. O'Keeffe and O. M. Yaghi, *Science*, 2008, **319**, 939; (c) X. D. Chen, H. F. Wu, X. H. Zhao, X. J. Zhao and M. Du. *Cryst. Growth Des*., 2007, **7**, 124; (d) M. Du, Z. H. Zhang, Y. P. You and X. J. Zhao, *CrystEngComm*, 2008, **10**, 306.; (e) R. P. Feazell, C. E. Carson and K. K. Klausmeyer, *Inorg. Chem*., 2006, **45**, 2627.
(15) G. M. Sheldrick, *SHELXL-97*: program for structure determination and Refinement: University of Göttingen: Göttingen, 1997.
(16) G. M. Sheldrick, SADABS 2.05; University of Göttingen: Germany, 2002.
(17) S. R. Batten, S. M. Neville and D. R. Turner, Coordination Polymers: Design, Analysis and Application, Royal Society of Chemistry, Cambridge, 2008, Chapter 3.
(18) (a) B. F. Hoskins, R. Robson and D. A. Slizys, *Angew. Chem., Int. Ed. Engl*., 1997, **36**, 2336; (b) J.Yang, J. F. Ma, S. R. Batten and Z. M. Su, *Chem. Commun*., 2008, 2233; (c) G. H. Wang, Z. G. Li, H. Q. Jia, N. H. Hu and J. W. Xu, *Cryst. Growth Des*., 2008, **8**, 1932.
(19) (a) D. M. L. Goodgame, S. Menzer, A. M. Smith and D. J. Williams, *Angew. Chem., Int. Ed. Engl*. 1995, **34**, 574; (b) F. Luo, Y. T. Yang, Y. X. Che and J. M. Zheng, *CrystEngComm*, 2008,**10**, 981; (c) X. Y. Cao, Y. G. Yao, S. R. Batten, E.Ma, Y.Y. Qin, J.. Zhang, R. B. Zhang and J. K.Cheng, *CrystEngComm*, 2009, 11, 1030; (d) J. Q. Liu, Y. Y. Wang, S. R. Batten.; H. Sakiyama and D. Y. Ma, *Inorg. Chem. Commun*., 2012, **19**, 27.
(20) M.O'Keeffe, M. A.Peskov, S. J. Ramsden and O. M. Yaghi, *Acc. Chem. Res*., 2008, **41**, 1782.
(21) (a) B. F. Abrahams, M. J. Hardie, B. F. Hoskins, R.Robson and E. E. Sutherland, *J. Chem. Soc., Chem. Commun*., 1994, 1049; (b) D. L. Long, J. Hill, J. Blake, N. R. Champness, P. Hubberstey, C.Wilson and M. Schröder, *Chem. Eur. J*., 2005,**11**, 1384
(22) D. Chen, Y. J. Liu, Y. Y. Lin, J. P. Zhang and X. M. Chen, *CrystEngComm*, 2011,**13**, 3827.
(23) P. Liu, Y. Y. Wang, D. S. Li, H. R.Ma, Q. Z. Shi, Q. G. H. Lee and S. M.Peng, *Inorg. Chim. Acta*., 2005, **358**, 3807.
(24) (a) D. R. Xiao, Y. G. Li, E. B. Wang, L. L.Fan,H. Y. An, Z. M.Su and L.Xu, *Inorg. Chem*., 2007, **46**, 4158; (b) H. Y. Wang, S. Gao, L.H. Huo, S. W. Ng and J. G. Zhao, *Cryst. Growth Des*. 2008, **8**, 665; (e) X. M. Zhang, R. Q. Fang and H. S. Wu, *CrytstEngComm*, 2005, **7**, 96; (f) C. J. Li, S. Hu, W.Li, C. K. Lam, Y. Z. Zheng and M. L Tong, *Eur. J. Inorg. Chem*., 2006, 1931.
(25) (a) J. Q. Liu, J. Wu, Y. Y. Wang and D. Y. Ma, *J. Coord. Chem*. 2012, **65**, 1303; (b) J. Q. Liu, Y. Y. Wang, T. Wu and J.Wu, *CrystEngComm*, 2012, **14**, 2906.
[26] C. Y. Sun, X. J. Zheng, S. Gao, C. L. Li and L.P. Jin, *Eur. J. Inorg. Chem*. 2005, 4150.
[27] P. Román, C.Guzmán-Miralles, A.Luque, J. I. Beitia, J. Cano, F.LIoret, M. Julve and S. Alvarez, *Inorg. Chem*., 1996, **35**, 3741; (b) G. Aromi, A. R.Bell, M.Helliwell, J. Raftery, S. J. Teat, G. A.Timco, O. Roubeau and R. E. P. Winpenny, *Chem. Eur. J*., 2003, **9**, 3024; (c) W. Luo, X. T. Wang, G. Z. Chen, S. Gao and Z. P. Ji, *Inorg. Chem. Common*. 2008, **11**, 769.
[28] H. Sakiyama, *J. Comp. Chem*., Jpn. **2007**, 6, 123.
[29] (a) S. Z. Wang, D. R. Zhu, Y. Xu, J. Yang, X. Shen, J. Zhou, N. Fei, X. K. Ke and L. M. Peng, *Crystal Crowth Des*., 2010, **10**, 887; (b) T. Kawata, H.Uekusa, S.Ohba, T. Furukawa, T.Tokii, Y. Muto and M. Kato, *Acta Crystallogr., Sect. B*., 1992, **48**, 253; (c) D. P. Martin, R. J. Staples and R. L. LaDuca, *Inorg. Chem*., 2008, **47**, 9754.

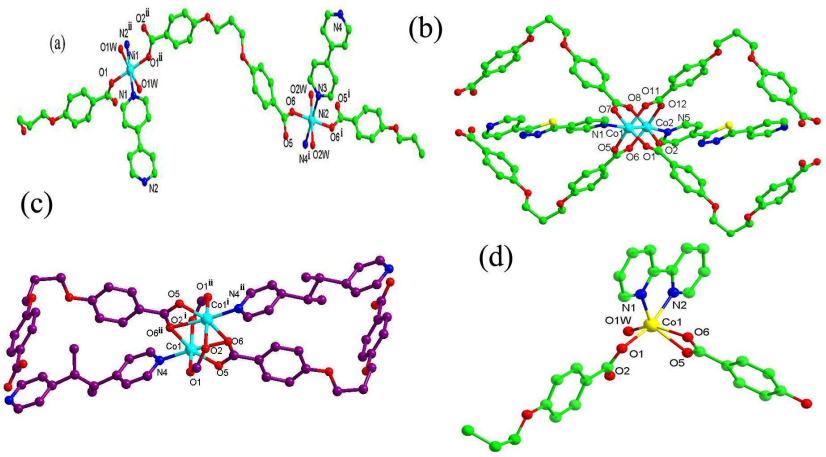

Fig 1. The structures of compounds: (a) the coordination geometry of the metal centre and the ligand geometry in **1** (symmetric code: (i) –x+3/2, -y+1, z; (ii); -x, y, -z+1/2); (b) the coordination geometry of the metal centre and the ligand geometry in **2**; (c) the coordination geometry of the metal centre and the ligand geometry in **3** (symmetric code: (i) -x-1, -y+2, z; (ii); x-1, y+1, z); (c) the coordination geometry of the metal centre and the ligand geometry in **4**.

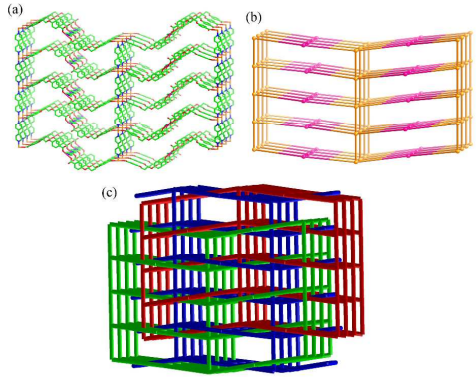

Fig. 2 (a) The 3D coordination polymer of **1**. Hydrogen atoms and water molecules are omitted for clarity; (b) a schematic representation of the $CdSO_4$ (**cds**) network topology; only the metal atoms are shown; links represent the bridging ligands; and (c) the three interpenetrating networks.

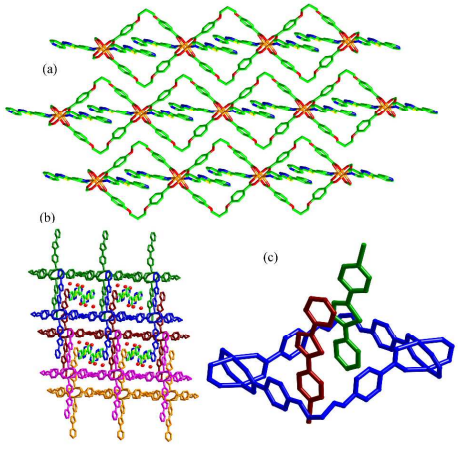

Fig 3. The structure of compound **2**: (a) A single layer of 1D chains in the structure of **2**; (b) Interdigitation of adjacent layers of chains, and the formation of channels contains intercalated

water and bpt molecules; (c) The penetration of one chain loop by two bcp ligands from adjoining chains; the metal atom coordinated to the bcp ligand is included in this view to indicate the coordinated and uncoordinated pyridyl groups.

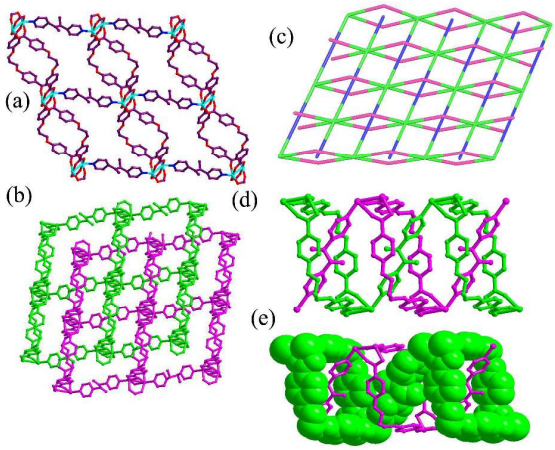

Fig. 4 (a) a perspective view of the sheet-like structure; (b) schematic view of two-interpenetrated network; (c) a representation of interlocked nets; (d) the polyrotaxane motif; (e) the polycatenane motif in **3**.

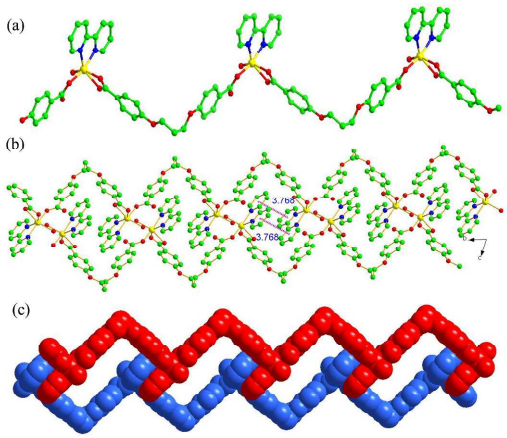

Figure 5: The structure of compound **4**: (a) viewing of the 1D helical chain; (b) the 2D supramolecular sheets formed by aromatic stacking interactions; and (c) optional view of zipperlike double-stranded chains.

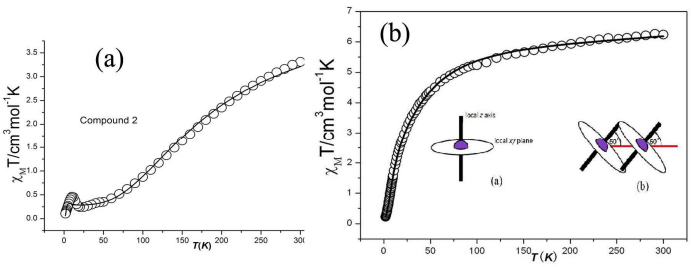

Fig. 6 (a) Plots $\chi_M T$, versus T for **2,** and (b) plots $\chi_M T$ versus T for **3**, solid lines represent fits to the data.

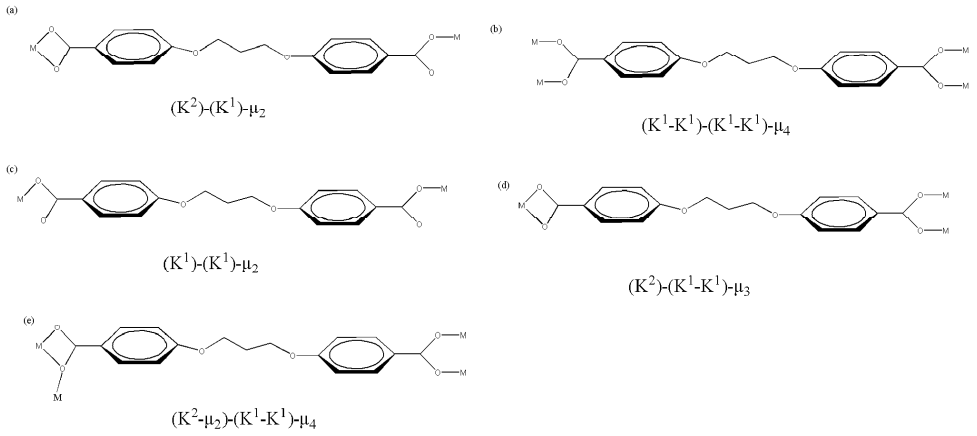

Scheme1. The kinds of coordinative modes for bcp ligand.

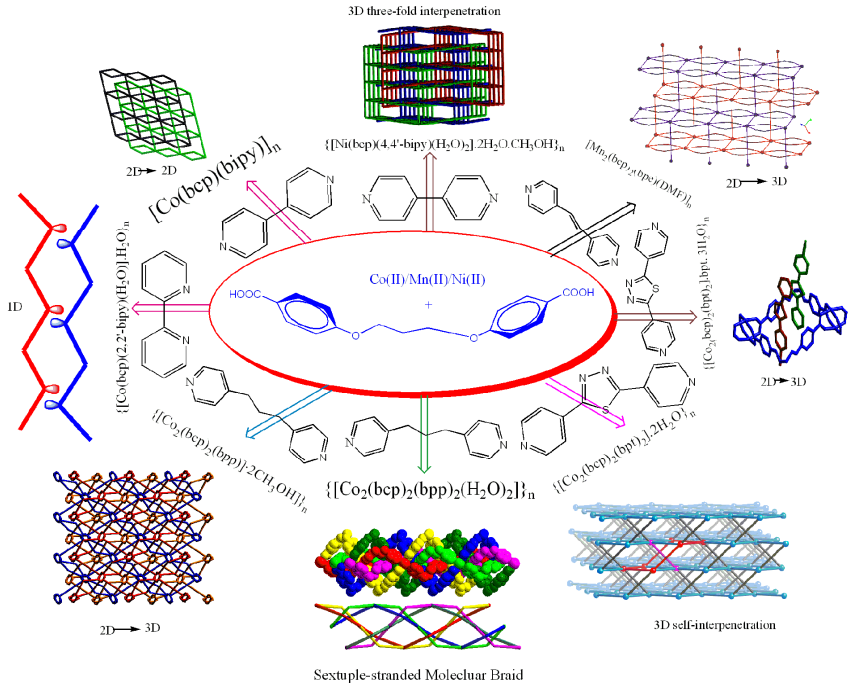

Scheme 2. Conclusion of the coordination chemistry of bcp ligand[11a,11e,19d, 25].

Table 1 the crystallographic data of **1**–**4**.

Complex	**1**	**2**	**3**	**4**
Empirical formula	$C_{54}H_{59}N_4Ni_2O_{19.5}$	$C_{70}H_{56.58}Co_2N_{12}O_{14.29}S_3$	$C_{48}H_{44}Co_2N_2O_{12}$	$C_{27}H_{26}CoN_2O_8$
Formula mass	1193.48	1508.55	958.71	565.43
Crystal system	Orthorhombic	Triclinic	Monoclinic	Triclinic
Space group	*Pcca*	*P*$\bar{1}$	*P* $2_1/c$	*P*$\bar{1}$
a [Å]	23.423(4)	14.079(5)	13.0721(8)	9.6092(9)
b [Å]	11.2363(19)	14.669(5)	8.1857(4)	10.695(11)
c [Å]	22.563(4)	19.559(6)	21.867(3)	13.436(3)
α [˚]	90	108.878(5)	90	70.763(2)
β [˚]	90	92.031(7)	107.835(8)	87.595(2)
γ [˚]	90	116.314(5)	90	72.381(2)
V [Å^3]	5938.3(18)	3349.0(19)	2227.4(4)	1240.0(2)
Z	4	2	2	2
d_{calcd} [g·cm^{-3}]	1.335	1.497	1.429	1.514
μ [mm^{-1}]	0.713	0.666	0.811	0.748
F(000)	2592	1557	992	586
θ Range [°]	1.74–25.19	1.65–25.10	2.67–27.10	1.60–25.22
Reflections collected	28705	16723	10846	6740
$R_{(int)}$	0.0841	0.0941	0.1004	0.0222
R_1, wR_2 [$I>2\sigma(I)$]	0.0626, 0.1711	0.0594, 0.0823	0.0747, 0.1255	0.0447, 0.1104
R_1, wR_2 (all data)	0.1124, 0.1917	0.0645, 0.2876	0.1537, 0.1658	0.0702, 0.1165

Table 2. Selected bond distances (Å) and angles (°)

1			
Ni2-O2W#1	2.109(4)	Ni2-O6#1	2.052(3)
Ni2-N3	2.118(5)	Ni2-N4	2.089(5)
Ni1-O1#2	2.027(3)	Ni1-O1W#2	2.118(3)
Ni1-N1	2.088(5)	Ni1-N2	2.076(5)
O2W-Ni2-O2W#1	179.1(2)	O6-Ni2-O6#1	178.80(17)
N3-Ni2-N4	180	O6-Ni2-N4	90
O1-Ni1-O1#2	179.96(19)	O1W-Ni1-O1W#2	176.37(17)
N1-Ni1-N2	180	O1-Ni1-N1	90
Symmetric code: #1: –x+3/2, -y+1, z; #2: -x, y, -z+1/2			
2			
Co1-O1	2.053(5)	Co1-O5#1	2.017(4)
Co1-O7	2.153(5)	Co1-O11#2	1.983(4)
Co1-N1	2.095(5)	Co2-O2	2.090(5)
Co2-O6	1.966(5)	Co2-O8	2.001(4)
Co2-O12	2.002(5)	Co2-N5	2.053(5)
O1-Co1-O5	92.3(2)	O1-Co1-O7	167.6(2)
O5-Co1-O7	85.67(18)	O5 -Co1-O11	164.1(2)
O5-Co1-N1	88.8(2)	O6-Co2 -O12	165.0(2)
Symmetric code: #1: x+1, y+1, z; #2: x-1, y-1, z			
3			
Co1-O2#1	1.996(4)	Co1-O1#2	2.006(4)
Co1-N4#2	2.074(4)	Co1-O5	2.087(4)
Co1-O6#2	2.286(3)	Co1-Co1#1	2.8790(14)
O1-Co1-O2	161.14(15)	N4-Co1-O6	172.56(16)
N4-Co1-O5	112.15(16)	O1-Co1-O5	96.63(15)
Symmetric code: #1: -x-1, -y+2, -z+1; #2: x-1, y+1, z			
4			
Co1-O1	2.032(2)	Co1-O1W	2.0886(19)
Co1-N1	2.109(3)	Co1-N2	2.125(2)
Co1-O5#1	2.298(2)	Co1-O6#1	2.160(2)
O1 -Co1-O1W	88.69(8)	O1-Co1-N1	90.49(9)
O1-Co1-N2	163.93(10)	O1-Co1-O5#1	104.43(9)
O1 -Co1-O6#1	93.00(9)	O5-Co1-N1	146.37(8)
Symmetric code: #1: x-1, y-1, z			